ISIJ International, Vol. 46 (2006), No. 2, pp. 316–324

# Strain-induced Transformation Behaviour of Retained Austenite and Tensile Properties of TRIP-aided Steels with Different Matrix Microstructure

Monideepa MUKHERJEE,[1)] Omkar Nath MOHANTY,[2)] Shun-ichi HASHIMOTO,[3)] Tomohiko HOJO[4)] and Koh-ichi SUGIMOTO[5)]

1) TATA Steel, Jamshedpur-831001, India, currently at IIT Kharagpur, India. 2) Formerly at TATA Steel, Jamshedpur-831001, India. 3) CBMM Asia Co. Ltd., 4-1-4, Akasaka, Minato-ku, Tokyo 107-0052 Japan.
4) Graduate Student of Shinshu University, 4-17-1, Wakasato, Nagano 380-8553 Japan.
5) Faculty of Engineering, Shinshu University, 4-17-1, Wakasato, Nagano 380-8553 Japan. E-mail: sugimot@shinshu-u.ac.jp

(*Received on September 27, 2005; accepted on November 8, 2005*)

The effects of strain rate and temperature on the strain induced transformation behaviour of retained austenite and hence mechanical properties of TRIP-aided steels with annealed martensite (AM), bainitic ferrite (BF) and polygonal ferrite (PF) matrix microstructures were examined. For this, tensile tests were carried out at four different strain rates varying from $3.33\times10^{-5}\,s^{-1}$ to $3.33\times10^{-2}\,s^{-1}$ at room temperature and at 150°C. Additional intermittent tests were carried out at intermediate strain rates to estimate the extent of strain induced transformation of austenite to martensite using X-ray diffraction analysis. Tensile strength (TS) decreased with strain rate at both temperatures, though the TS at 150°C was lower for all steels except for BF steel tested at $3.33\times10^{-5}\,s^{-1}$. The total elongation (TEL) for PF steel significantly improved at 150°C at all strain rates, with a maximum of 78 % obtained at $3.33\times10^{-3}\,s^{-1}$, the corresponding TS being 930 MPa. A similar effect was seen in AM steels tested at $3.33\times10^{-3}\,s^{-1}$ and $3.33\times10^{-4}\,s^{-1}$. However, in BF steel, higher temperature had a detrimental effect on TEL, especially at strain rates of $3.33\times10^{-2}\,s^{-1}$ and $3.33\times10^{-3}\,s^{-1}$.

KEY WORDS: microstructure; ductility; TRIP; retained austenite; annealed martensite; bainitic ferrite; morphology; tensile property.

## 1. Introduction

Low alloy TRIP[1)]-aided steels are being considered as promising materials for autobody applications as they offer an excellent combination of strength and ductility at affordable costs. The high strength thinner gauge sheet steel enables reduced fuel consumption and emissions by reducing passenger car weight. Better passenger safety is also ensured by the improved crash-worthiness.[2)]

These steels typically have a microstructure consisting of ferrite, bainite and retained austenite. The presence of retained austenite leads to better mechanical properties that can be attributed to its transformation to martensite on straining.[3)] To guarantee high formability, the retained austenite should possess what is called optimal stability which enables it to undergo progressive transformation, which in turn leads to a more continuously increasing strain hardening exponent as the TRIP effect is spread out over a larger strain range.[4)] Stability of austenite depends on a number of factors *viz*. chemical composition, annealing parameters, morphology and size of retained austenite and forming conditions (test temperature, strain, strain rate and stress state).[5)]

In recent years, three kinds of TRIP-aided steels with different matrix microstructures have been developed in response to the complex formability requirements of the present day auto-body manufacturers.[6–8)] As the retained austenite morphology and content in the three steels are also different, it is expected that its strain-transformation behavior is influenced by forming conditions. So, in this work an attempt has been made to understand for the first time, the effects of strain rate and temperature on the strain induced transformation behaviour of retained austenite and hence mechanical properties of TRIP-aided steels with different matrix microstructures.

## 2. Experimental Procedure

The chemical composition of the steel used in this study is given in **Table 1**. Al was added for increasing carbon concentration of retained austenite[9)] while complex addition of Nb+Mo was incorporated to bring about precipitation hardening by fine NbMoC precipitates.[10)] The steel was supplied by Kobe Steel Ltd. in the form of vacuum melted, cold rolled sheets of 1.2 mm thickness. Tensile specimens of 50 mm gauge length and 12.5 mm gauge width (ASTM E8) were machined from the as-received sheets parallel to the rolling direction. These were subsequently heat treated

**Table 1.** Chemical composition.

| | C | Si | Mn | P | S | Al | Nb | Mo | N | O |
|---|---|---|---|---|---|---|---|---|---|---|
| Composition (mass %) | 0.40 | 0.49 | 1.48 | 0.015 | 0.0009 | 0.96 | 0.024 | 0.10 | 0.0005 | <0.0006 |

in salt baths using three different heat treatment regimes shown in **Fig. 1**, to obtain three different matrix morphologies. The austempering temperature of 450°C was chosen as preliminary tests conducted at this temperature resulted in maximum volume fraction of retained austenite. The first treatment (Fig. 1(a)) results in an annealed martensite matrix and the steel will be hence forth referred to as AM steel, the second treatment (Fig. 1(b)) results in a steel with bainitic ferrite matrix microstructure and will be referred to as BF steel and the third treatment (Fig. 1(c)) results in the conventional TRIP-aided steel microstructure with polygonal ferrite matrix which will be referred to as PF steel.

Tensile tests were carried out at room temperature (RT) and at 150°C on a hard tensile testing machine at mean strain rates varying from $3.33\times10^{-5}\,s^{-1}$ to $3.33\times10^{-2}\,s^{-1}$ (*i.e.* cross head speeds varying from 0.1 mm/min to 100 mm/min). Intermittent tensile tests were also carried out using duplicate samples up to five strain levels, at typical strain rates, to determine strain induced transformation behaviour of austenite. For this, volume fraction of retained austenite was estimated by X-ray diffractometry using Cu-K$\alpha$ radiation. The calculations were based on the integrated intensities of $(200)_\alpha$, $(211)_\alpha$, $(200)_\gamma$, $(220)_\gamma$ and $(311)_\gamma$ diffraction peaks.[11] Specimens were prepared from as-heat treated samples as well as the shoulder (grip) portion of the tensile specimens for estimating the initial retained austenite characteristics. It was assumed here that the shoulder section undergoes very little strain and hence the original amount of austenite retained after heat treatment, is preserved. On the other hand, specimens prepared from the gauge section of the tensile samples were used to analyse the characteristics of the untransformed austenite left behind after a certain amount of strain.

Carbon concentration of retained austenite was evaluated from the lattice constant measured from $(200)_\gamma$, $(220)_\gamma$ and $(311)_\gamma$ diffraction peaks using the equation proposed by Dyson and Holmes.[12]

Optical microscopy was used to examine the LePera etched microstructures of the as-heat treated samples.

## 3. Results

### 3.1. Microstructure and Retained Austenite Characteristics

The optical micrographs of the as-heat treated steels are shown in **Fig. 2**. The AM steel consists of fine annealed martensite lath matrix (grey) and inter lath second phase consisting of plate like and blocky retained austenite (white) as well as carbide free bainite (black). The BF steel has bainitic ferrite lath matrix (grey-black) with inter lath retained austenite (white). The microstructure appears to be somewhat coarser than the AM steel, but like AM steel, the retained austenite has both blocky as well as plate like morphologies. The PF steel displays fine network microstructure of polygonal ferrite matrix (grey). The second phase seems to consist of bainite (black), and a large amount of retained austenite/martensite (white).

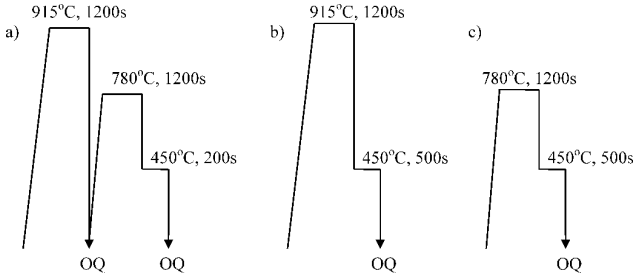


**Fig. 1.** Heat treatment schedules for producing TRIP-aided steels with (a) annealed martensite matrix (AM), (b) bainitic ferrite matrix (BF) and (c) polygonal ferrite matrix (PF). ("OQ" represents oil quenching).

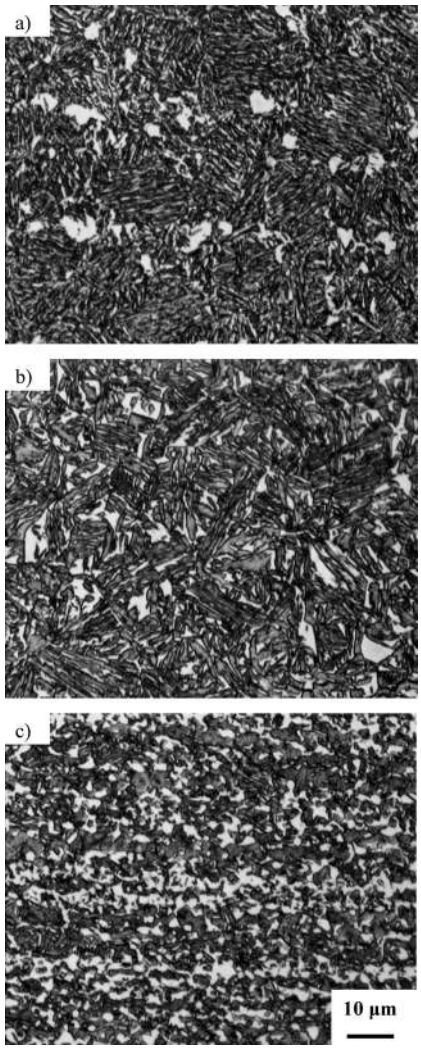


**Fig. 2.** Optical micrographs of (a) AM steel, (b) BF steel and (c) PF steel in the as-heat treated condition (LePera etching).

The initial retained austenite characteristics are listed in **Table 2**. AM steel is found to have a high amount of carbon enriched retained austenite. In BF steels, the initial retained austenite volume fraction ($f_{\gamma_o}$) is lower but its carbon concentration ($C_{\gamma_o}$) is high and hence its stability is likely to be

similar to that in AM steels. The initial retained austenite in PF steel has very low carbon concentration which is hence likely to be more unstable compared to AM or BF steels. The numerals in the parentheses indicate the average retained austenite in the shoulder sections of PF steel samples tested at RT which is much less than that in the as-heat treated sample. The same is not mentioned for AM and BF steels as retained austenite content is nearly the same in the shoulder sections and the as heat-treated samples. The reason for this discrepancy will be discussed in subsequent sections.

### 3.2. Mechanical Properties

The engineering stress–strain curves for the three steels tested at different strain rates and temperatures are shown in **Fig. 3**. While fine serrations are observed during low strain rate tests ($3.33\times10^{-4}\,s^{-1}$ and $3.33\times10^{-5}\,s^{-1}$) at RT, the fluctuations are much more prominent at 150°C, with intense serrations near the yield point. Load drops continue even up to peak load. However, as strain rate increases the intensity of fluctuations decreases and is nearly absent at $3.33\times10^{-2}\,s^{-1}$. PF steels tested at RT have a distinct yield plateau at all strain rates, while at 150°C, only high strain rate ($3.33\times10^{-2}\,s^{-1}$ and $3.33\times10^{-3}\,s^{-1}$) flow curves have a yield point. In BF steels, on the other hand, only the test conducted at $3.33\times10^{-5}\,s^{-1}$, at 150°C generated a yield point whereas in AM steel the same is observed only for the test conducted at RT at $3.33\times10^{-2}\,s^{-1}$.

Deformation bands were observed in all steel samples tested at strain rates of $3.33\times10^{-4}\,s^{-1}$ and $3.33\times10^{-5}\,s^{-1}$ at 150°C. The bands originated from one end of the gage length and were oriented at an angle of ~45° to the tensile axis and then at higher strains two sets of mutually perpendicular shear bands were observed. **Figure 4** shows the shear bands formed in BF steel samples tested at 150°C at a strain rate of $3.33\times10^{-5}\,s^{-1}$ strained up to (a) 2% and (b) 10.5 % nominal strain.

**Figure 5** shows the effect of strain rate on yield strength (YS), tensile strength (TS) and yield ratio (YR) of the three steels tested at RT and 150°C. At RT, PF steel has the lowest yield strength (YS) and the highest tensile strength (TS) resulting in the lowest yield ratio. At 150°C, YS of AM and BF steels is lower than the corresponding RT values, but the effect is opposite in the case of PF steels which has higher YS at 150°C. TS for all three steels is lower at 150°C (except for BF steel tested at $3.33\times10^{-5}\,s^{-1}$). Increasing strain rate clearly causes decrease in TS at both temperatures. At 150°C, YS of AM and BF steels decreases

**Table 2.** Initial retained austenite characteristics of the as-heat treated steels.

| Steel Type | $f_{\gamma o}$ | $C_{\gamma o}$ (mass %) | $f_{\gamma o}$ x $C_{\gamma o}$ (mass %) |
|---|---|---|---|
| AM | 0.20 | 1.08 | 0.22 |
| BF | 0.15 | 1.12 | 0.17 |
| PF | 0.25(0.14*) | 0.77 | 0.19 |

* Shoulder section of specimens tested at RT

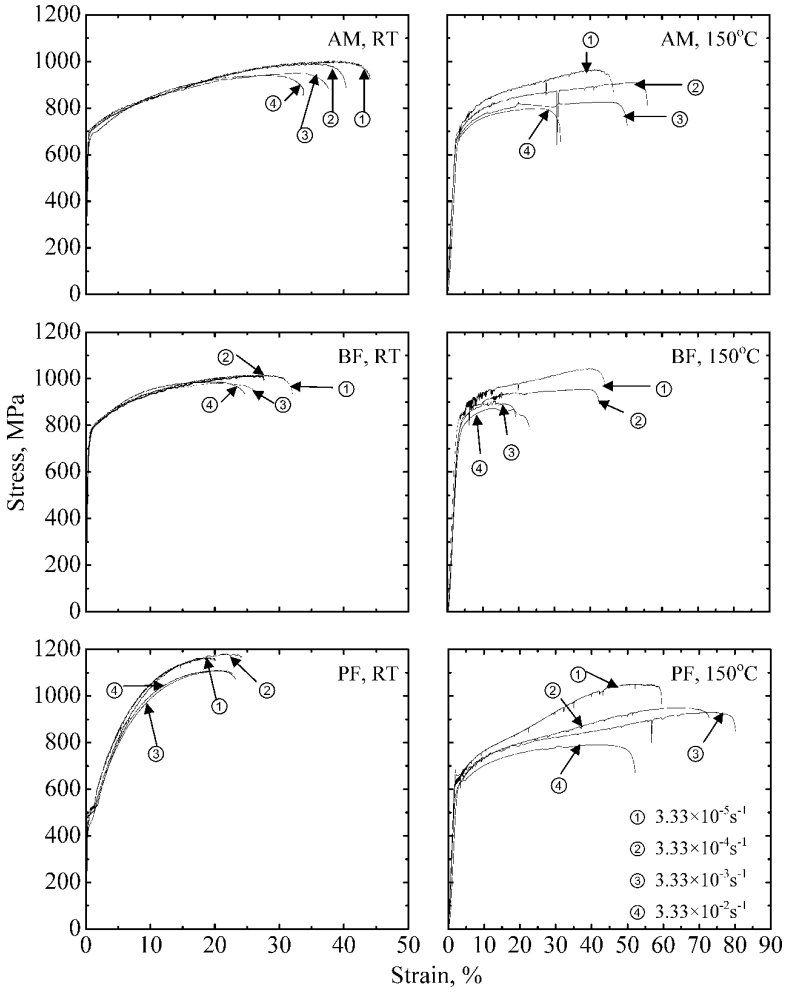


**Fig. 3.** Engineering stress–strain plots for AM, BF and PF steels.

slightly with strain rate, but at RT, the effect is not very clear. YR of PF steels is higher than at RT but in AM and BF steels YR is almost same as that at RT.

**Figure 6** shows the effect of strain rate on total elongation (TEL) and strength ductility balance (TS×TEL). At RT, AM steel has the highest and PF steel has the lowest TEL at all strain rates. Moreover, in AM and BF steels, TEL decreases with increasing strain rate. But in PF steels, the effect of strain rate is not so clear. At 150°C, TEL of PF steel significantly increases and reaches a maximum of 78% at $3.33\times10^{-3}\,s^{-1}$ (similar to TWIP[13] steels). In AM steels also, TEL at 150°C is higher than the corresponding RT values at intermediate strain rates of $3.33\times10^{-3}\,s^{-1}$ and $3.33\times10^{-4}\,s^{-1}$. In BF steels, TEL at $3.33\times10^{-4}\,s^{-1}$ and $3.33\times10^{-5}\,s^{-1}$ is higher than the corresponding RT values, but as strain rate increases, TEL decreases and is actually lower than the RT values at strain rates of $3.33\times10^{-2}\,s^{-1}$ and $3.33\times10^{-3}\,s^{-1}$. AM steel has the best TS×TEL combination (43.5 GPa%) at RT at a strain rate of $3.33\times10^{-5}\,s^{-1}$, while at 150°C, PF steel exhibits the best combination (72.3 GPa%) at $3.33\times10^{-3}\,s^{-1}$.

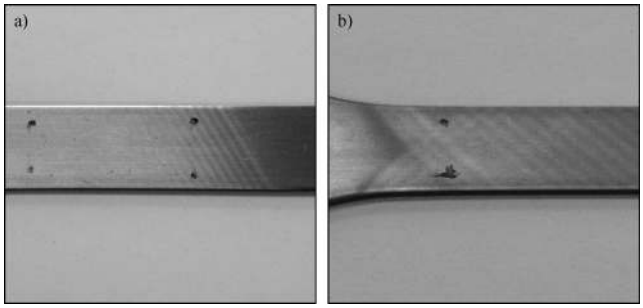


**Fig. 4.** Shear band formation in BF steel samples tested at 150°C at $3.3\times10^{-5}\,s^{-1}$ up to (a) 2% and (b) 10.5% nominal strain.

The change in strain hardening rate ($d\sigma/d\varepsilon$) with true strain is shown in **Fig. 7**. At RT, PF steels have a very high strain hardening rate at low strains which decreases rapidly with increasing strain. On the other hand the strain hardening rate in BF and AM steels are lower and decrease gradually with strain. At 150°C, the strain hardening rate initially decreases with strain, but after a certain intermediate strain, it again increases, goes through a maximum and again decreases. This effect is particularly observed in AM and PF steels tested at strain rates ranging between $3.33\times10^{-3}\,s^{-1}$ and $3.33\times10^{-5}\,s^{-1}$ and BF steels tested at $3.33\times10^{-5}\,s^{-1}$. At $3.33\times10^{-2}\,s^{-1}$, the strain hardening rate gradually decreases with strain in AM and PF steels while rapidly decreasing in BF steels.

To analyze the above results further, intermittent tensile tests were conducted for all three steels at the lowest

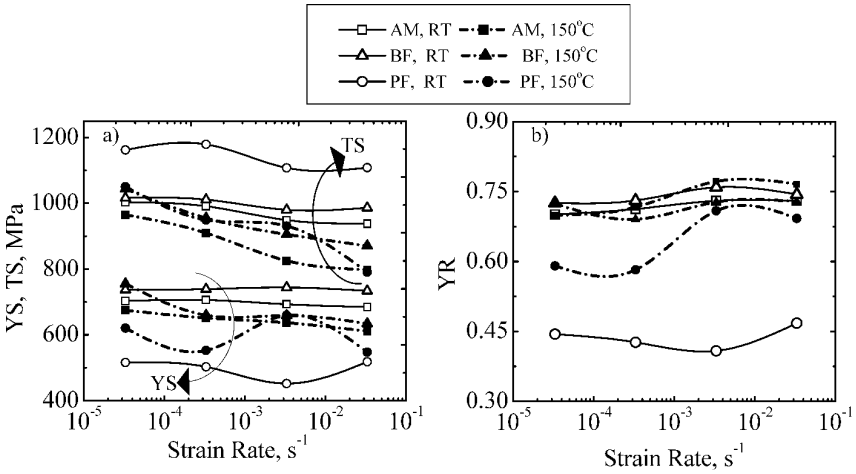


**Fig. 5.** Effect of strain rate on (a) yield strength (YS) and tensile strength (TS) and (b) yield ratio (YR).

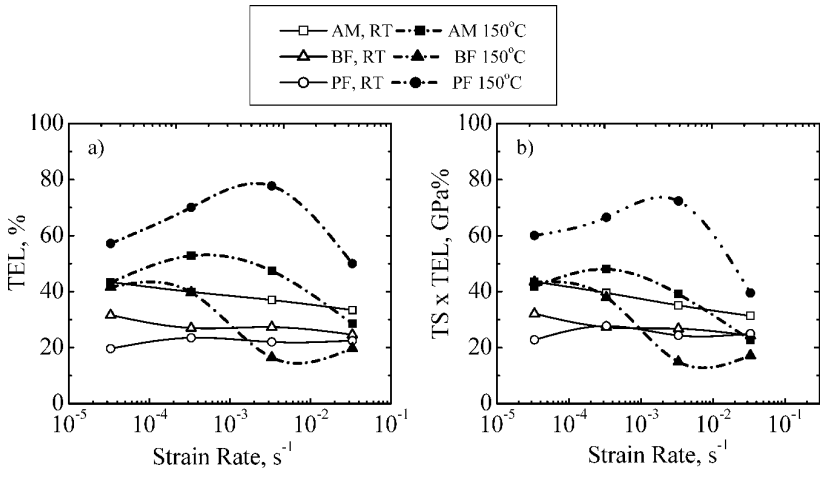


**Fig. 6.** Effect of strain rate on (a) total elongation (TEL) and (b) strength–ductility balance (TS×TEL).

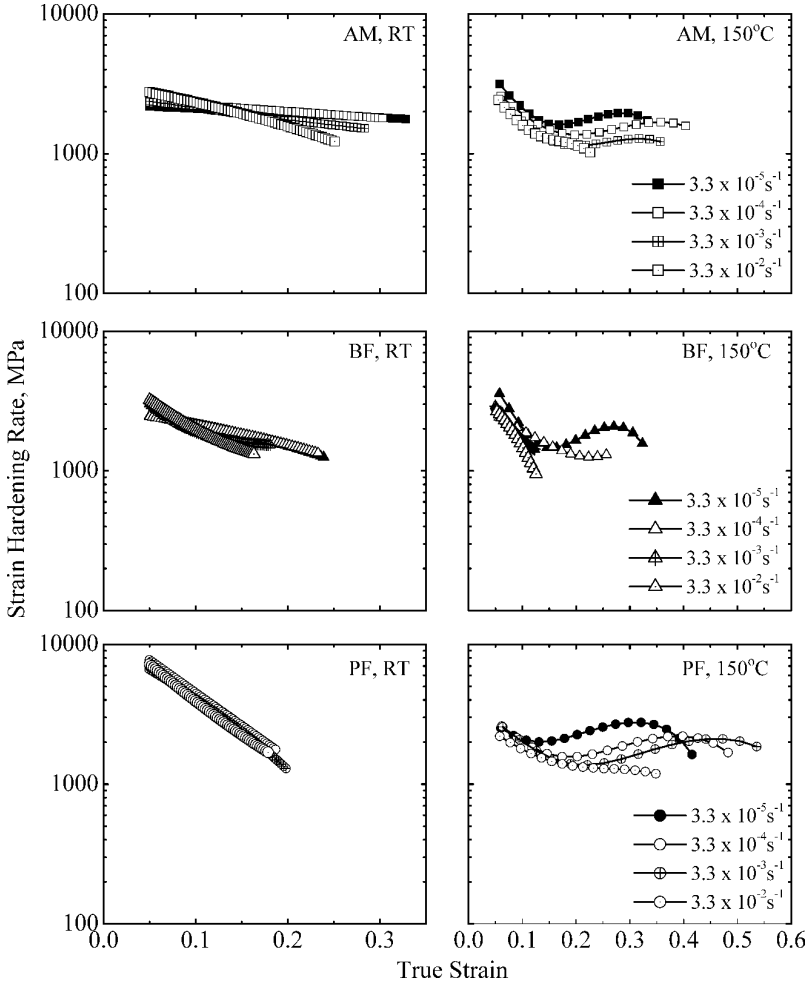


**Fig. 7.** Strain hardening rate–strain curves of AM, BF and PF steels.

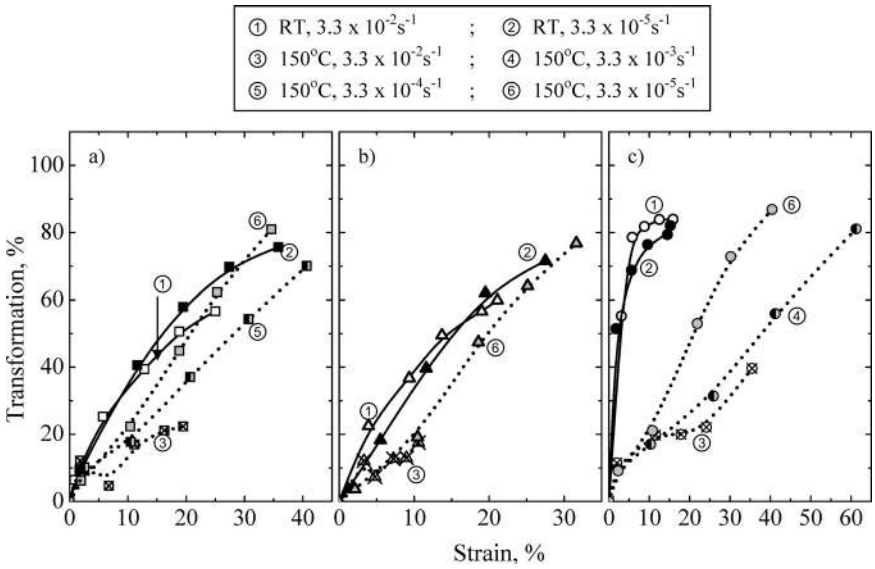


**Fig. 8.** Retained austenite transformation (%) as a function of strain in (a) AM, (b) BF and (c) PF steels.

($3.33\times10^{-5}\,s^{-1}$) and highest ($3.33\times10^{-2}\,s^{-1}$) strain rates, up to five strain levels, at both temperatures. Additionally, at 150°C, intermittent tensile tests were carried out at $3.33\times10^{-4}\,s^{-1}$, for AM steel and at $3.33\times10^{-3}\,s^{-1}$ for PF steel, as maximum TEL was recorded at these strain rates. All samples were then subjected to X-ray diffraction study to determine strain induced transformation behaviour of retained austenite.

### 3.3. X-ray Diffraction

**Figure 8** shows the retained austenite transformation (%) as a function of strain as determined from X-ray diffraction using the following equation:

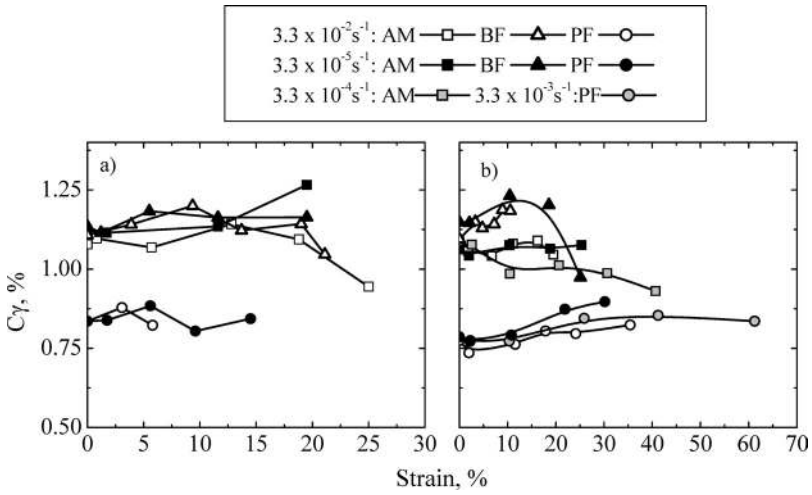


**Fig. 9.** Carbon content of untransformed austenite in steels tested at (a) RT and (b) 150°C as a function of strain.

$$\% \text{ Transformation} = \frac{f_{\gamma_o} - f_{\gamma,e}}{f_{\gamma_o}} \times 100 \quad \text{.....(1)}$$

where $f_{\gamma_o}$ is the initial retained austenite and $f_{\gamma,e}$ is the retained austenite which remains untransformed after a nominal strain of $e$%.

In PF steel, % transformation is much higher than in AM and BF steels, when tested at RT. Moreover, most of the transformation takes place at low strains, with the curves flattening out as strain increases, indicating low transformation at high strains. This effect is more prominent at the higher strain rate. In AM and BF steels, on the other hand, the transformation seems to be gradual and progressive at the low strain rate. At the higher strain rate, the transformation seems to shift to lower strains in BF steels. In AM steels also, % transformation increases at lower strains and decreases at higher strains on increasing the strain rate.

At 150°C, transformation is much slower compared to that at RT, the effect becoming more evident at higher strain rates. The effect of temperature is most striking in PF steels, in which austenite seems to have attained optimal stability at 150°C and hence is able to transform at a slow and progressive rate, leading to much higher TEL values.

Variation of the carbon content of untransformed retained austenite ($C_\gamma$) with strain is shown in **Fig. 9**. $C_\gamma$ seems to increase with increase in strain, especially at low strains (0–10%) in BF and PF steels tested at RT after which it appears to remain constant or even decrease. At 150°C, the $C_\gamma$ of PF steel continues to increase even up to high strain levels, whereas the trend for BF steel is similar to that at RT. However, the unusually low $C_\gamma$ measured at around 25% strain in the BF steel tested at $3.33\times10^{-5}\,s^{-1}$, could be due to some error as the steel had only around 5.6% untransformed austenite.[11] In AM steel, the carbon content hardly changes for samples tested at the lowest and highest strain rates at either temperature, but for the samples tested at 150°C at $3.33\times10^{-4}\,s^{-1}$, $C_\gamma$ decreases with strain. And for the RT test carried out at $3.33\times10^{-5}\,s^{-1}$, there is an increase in carbon content at around 20% strain.

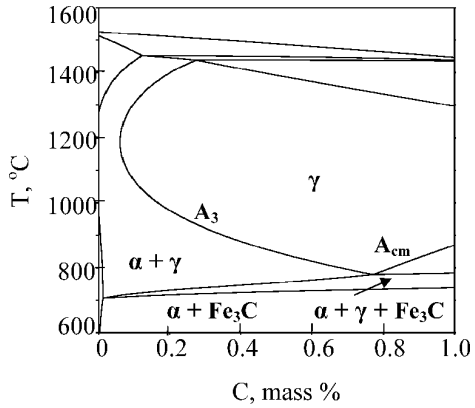


**Fig. 10.** Equilibrium diagram of Fe–C–0.5Si–1.5Mn–1.0Al system computed by Thermo-Calc.[14]

## 4. Discussion

### 4.1. Retained Austenite Stability

#### 4.1.1. Initial Retained Austenite Characteristics

The initial retained austenite in AM and BF steels possesses higher $C_{\gamma_o}$ than PF steels. Since the steel chemistry is the same, the difference arises due to the difference in heat treatment methodologies adopted. Considering the AM and PF steels first, there are mainly two differences in their respective heat treatments. Firstly, the AM steels are subjected to an additional austenitizing and oil quenching step prior to the conventional treatment of intercritical annealing and then austempering, and secondly, the austempering time in the case of the AM steel is shorter. From the equilibrium phase diagram of Fe–C–0.5Si–1.5Mn–1.0Al system computed by Thermo-Calc,[14] shown in **Fig. 10**, one can calculate using Lever Rule that ~54% austenite with ~0.73% carbon should form after intercritical annealing treatment at 780°C (assuming the reaction reaches equilibrium). If it is assumed that no ferrite forms during the subsequent cooling to the austempering temperature, the austenite has 0.73% carbon at the beginning of the austempering treatment also. During the isothermal holding supersaturated bainite forms as a first step. This supersaturation can be relieved by either partitioning of carbon to austenite or formation of carbides. Some amount of carbon may even remain trapped in the dislocated structure of the newly

formed bainite. Formation of carbides in Al–Si containing steel is difficult because of the low solubility of these elements in carbides.[15] Therefore, it is more likely that most of the carbon partitions to austenite. This partitioning can continue till the carbon of austenite reaches the composition given by the $T_o$ line,[15] which for 0.2C, 1.5Mn, 0.6Si, 1.0Al containing steel is around 1.35%.[9] The relatively high carbon content of austenite at the beginning of the austempering treatment (0.73%) indicates a slow transformation kinetics. This should be however applicable to both steels. Another factor which therefore needs to be considered is the difference in morphologies of the intercritical austenite in the two steels. An earlier study[16] on the reverse transformation mechanism of martensitic stainless steel showed that at high reverse transformation temperatures film like austenite is formed between laths of martensite and small granular austenite is formed inside the laths. In the case of AM steels, therefore the austenite should possess a similar morphology after intercritical annealing. In PF steels on the other hand the austenite should have a relatively more blocky structure. Jacques[17] has shown that when the austenite grain size is small, the bainite transformation starts early but proceeds at a slower rate. This is due to the fact that the higher grain boundary area associated with smaller grains, results in an enhanced nucleation rate. Considering the above facts, the high $C_{\gamma_o}$ of AM steel (1.08%) suggests that the relatively short austempering time of 200 s is sufficient for bainite transformation to start and progress to a considerable extent as the austenite is of smaller size. In the case of PF steel however, the larger grain size of austenite delays the start of transformation and hence even after austempering for 500 s, extent of transformation is quite low resulting in the low $C_{\gamma_o}$ of PF steel.

For producing BF steels, the intercritical annealing treatment is eliminated altogether. After austenitizing, the steel is directly cooled to the austempering temperature at which the austenite has 0.4% carbon (though some proeutectoid ferrite could form during cooling and increase the carbon content of austenite). This lower carbon content of austenite at the beginning of the austempering treatment suggests faster transformation kinetics and the higher holding time of 500 s, enables more complete transformation of austenite to carbide free bainite, resulting in the higher carbon concentration of austenite.

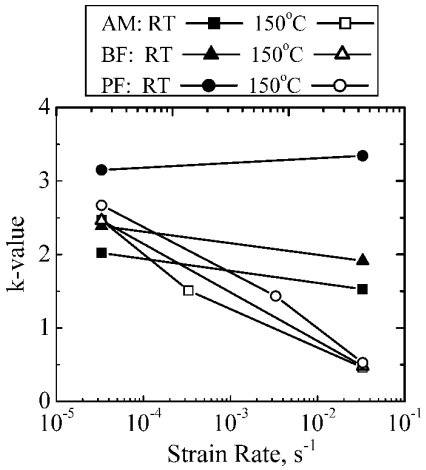


**Fig. 11.** Strain rate dependence of *k*-value in AM, BF and PF steels, tested at RT or 150°C.

4.1.2. Effect of Forming Conditions

As mentioned earlier, stability of retained austenite, is decided by the carbon content, morphology and size of the austenite itself and the morphologies of the other microstructural constituents. External conditions like test temperature and strain rate also affect stability. Among all these factors the most important factor however is the carbon content of austenite.[18]

The retained austenite in PF steels is likely to be relatively unstable as its carbon content is quite low. The high *k*-value[4] of PF steel at room temperature (**Fig. 11**) further corroborates this argument. This *k*-value as determined from the following equation is often used to describe the stability of retained austenite.

$$\log f_{\gamma,\varepsilon} = \log f_{\gamma_o} - k\varepsilon \quad \text{.....(2)}$$

where $f_{\gamma,\varepsilon}$ is the retained austenite which remains untransformed after a true strain of $\varepsilon$.

Figure 11 also shows the variation of *k*-value with strain rate for the three steels tested at different temperatures. The *k*-value decreases with temperature especially at higher strain rates. In PF steels however, this effect is seen at all strain rates.

The effect of temperature on retained austenite stability to martensitic transformation can be understood from **Fig. 12** which illustrates the various transformation mechanisms at different temperatures. When stress (less than yield stress of the parent phase) is applied, at temperatures higher than $M_s$, stress assisted nucleation of martensite occurs on pre-existing nucleation sites (at which spontaneous transformation would have occurred on cooling below $M_s$). Beyond a

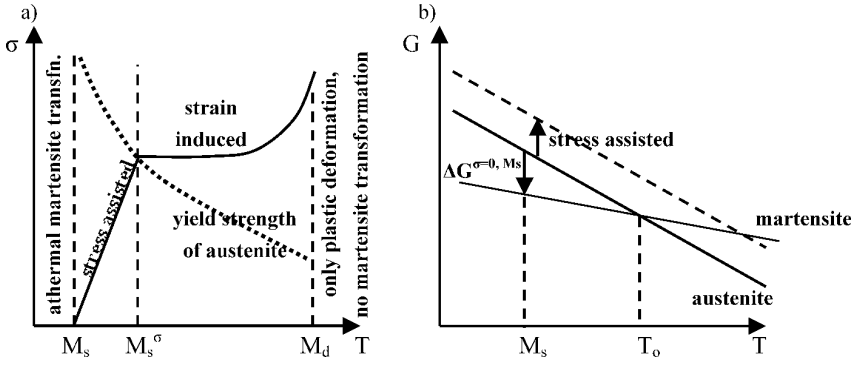


**Fig. 12.** Influence of temperature on (a) martensitic transformation mechanisms and (b) free energy change.[19]

temperature $M_s^\sigma$ at which the stress reaches the yield stress for slip in the austenite, new potent nucleation sites are generated which trigger the strain induced transformation of austenite to martensite. Therefore near $M_s^\sigma$ both modes operate. At temperatures above $M_d$, martensitic transformation can no longer be induced by deformation.[19)]

Lower carbon content of retained austenite in PF steel indicates higher $M_s$, $M_s^\sigma$ and $M_d$ temperatures. Moreover, the fact that at RT, austenite in the shoulder section of the PF steel samples (which are subject to very low strain) also undergo transformation indicates the possibility of stress induced transformation taking place, which suggests that $M_s^\sigma$>RT. When the test temperature is raised to 150°C, austenite can only undergo strain induced transformation as the test temperature is closer to $M_d$ and austenite stability is much higher (lower *k*-value).

Higher carbon content and hence lower $M_s$, $M_s^\sigma$ and $M_d$ temperatures, results in higher stability of the retained austenite in AM and BF steels. When test temperature is increased to 150°C, transformation is suppressed in these steels also, but the change is not as phenomenal as in PF steels. One reason for this could be that at both test temperatures only strain induced transformation takes place albeit the transformation is more suppressed at 150°C, as it is closer to the $M_d$ temperature.

The general observation of increasing stability of retained austenite (decreasing *k*-value) with increasing strain rate can be understood from the phenomenon of adiabatic heating which takes place at high strain rates, when the deformation rate is so fast that the thermal effects are not able to equilibrate with the surroundings.[20)] The resultant rise in temperature, increases the stability of retained austenite.

Over and above all the factors mentioned, the effect of morphology of the matrix constituents and the retained austenite itself, cannot be overlooked. The polygonal ferrite matrix is quite soft and does not resist transformation of austenite to martensite on straining, contributing to the observed low stability of retained austenite in PF steels. Whereas in AM and BF steels, the relatively hard matrix prevents transformation at an early stage. However, retained austenite in BF steels has lower stability compared to AM steels inspite of higher carbon content. This could be due to the small strength ratio of second phase to matrix in BF steels as a result of which the retained austenite is plastically strained during deformation.[8)] In AM steels, on the other hand medium strength ratio of second phase to matrix, results in higher stability of retained austenite.

Moreover, in BF and PF steels, the carbon concentration of austenite is not uniform as a result of which initially austenite with lower carbon content transforms leaving behind higher carbon containing stable austenite as is indicated by Fig. 9 which shows that the carbon content of the untransformed austenite in these steels increases with strain (especially from 0–10% strain). The nearly constant carbon content of untransformed austenite in AM steels suggests uniform carbon concentration in all austenite areas. This can be attributed to the morphology of intercritical austenite formed from the reverse transformation of martensite, in AM steels. This film shaped austenite is associated with a short mean free path or diffusion path.[8)]

### 4.2. Mechanical Properties

Mechanical properties of TRIP-aided steel are primarily influenced by the strain induced transformation behaviour of retained austenite. As pointed out in the previous section the retained austenite in PF steel is highly unstable. Therefore on deformation at RT, it starts transforming to martensite even under elastic strain and relatively low plastic strains as confirmed by XRD study, resulting in the formation of a large amount of martensite. This early formation of martensite may be responsible for the low yield stress at RT, as martensitic transformation results in the formation of new mobile dislocations in the surrounding matrix. At the same time, higher strength of martensite results in the extremely high strain hardening rate even at low strains. The failure of the austenite to undergo progressive transformation however causes rapid decrease in the strain hardening rate, resulting in the low TEL values. When the test temperature is raised to 150°C, mechanical stability of retained austenite is much higher and hence transformation is shifted to higher strains, as is observed in Figs. 8 and 11.

Sugimoto *et al*.[7)] have shown that when retained austenite has optimal stability, compressive long range internal stress in the matrix results due to the presence of untransformed retained austenite. This internal stress contributes to large strain hardening both in an early stage of straining and at high strains. On the other hand strain induced austenite to martensite transformation results in high strain hardening rate at higher strains, both factors contributing towards enhancing the TEL by postponing necking to higher strains. This explains the observed initial drop and subsequent increase in strain hardening rate with strain, and higher TEL in PF steels at 150°C.

In AM and BF steels, low strain rate tests at RT result in progressive transformation of the more stable austenite up to high strain levels resulting in a higher total elongation. However, the ductility of BF steels is lower than AM steels. One factor responsible for this is undoubtedly the lower amount of retained austenite present. Another important factor is the difference in the matrix microstructures. Bainitic ferrite is associated with a comparitively rapid decrease of strain hardening rate at an early stage, which is also responsible for the low ductility in BF steels.

The strain rate also has a considerable influence on the mechanical properties as observed in this study. In general, increasing strain rate tends to increase the flow stress of materials.[20)] But this trend is subject to accompanying temperature changes of the sample during the tensile test, one of the reasons for which could be adiabatic heating at high strain rates which results in the gradual increase of sample temperature with strain.[5)] This increase in temperature causes flow stress to decrease. But, by the time the sample reaches the yield point, the temperature rise due to adiabatic heating is quite low. So the opposing effects of higher strain rate and adiabatic heating result in a very small decrease (at the highest strain rate) in the yield stress of AM and BF samples tested at either temperature though at 150°C the lower yield stress values may be due to the temperature effect.

As the material undergoes more plastic strain beyond yielding considerable amount of adiabatic heating takes

place. As discussed in the previous section, extent of strain induced martensitic transformation of retained austenite decreases with increase in temperature above $M_s^{\sigma}$, and above $M_d$, there is no transformation at all. Therefore, adiabatic heating at high strain rate restricts the transformation to martensite at high strains, rendering the austenite stable to transformation. This phenomenon is observed at both test temperatures. Samples tested at high strain rates at RT undergo faster transformation up to ~10% strain compared to the lower strain rate test (Fig. 8), after which the transformation rate drops as sample temperature increases due to adiabatic heating. At 150°C also, the transformation begins at a relatively slow rate (due to high temperature) but at higher strains, the effect of strain rate becomes very clear, with very little transformation taking place at $3.3\times10^{-2}\,s^{-1}$. Considering the fact that the test temperature is already 150°C, any further heating results in sample temperature reaching very close to $M_d$, causing transformation to stop, leaving behind a large amount of untransformed austenite.

The lower TS at higher strain rates can be attributed to both the increased temperature due to adiabatic heating and the resultant lower amount of transformation at higher strains which results in lower amount of high strength martensite, the effect being more obvious at 150°C. However the concept of adiabatic heating used here to explain the effect of strain rate is purely speculative and hence further study is needed to have a clearer understanding of the underlying process.

## 5. Conclusions

The effects of temperature, strain and strain rate on the strain induced transformation behaviour and hence mechanical properties of TRIP-aided steels with different matrix microstructures were studied. The main conclusions that can be drawn from this study are:

(1) At RT, best strength–ductility balance of 43.5 GPa% was obtained in AM steel tested at $3.3\times10^{-5}\,s^{-1}$, while at 150°C, PF steel tested at $3.3\times10^{-3}\,s^{-1}$ had the best strength–ductility balance of 72.3 GPa%.

(2) Increasing test temperature resulted in suppression of retained austenite to martensite transformation, the effect being most striking in PF steel, in which optimal stability of retained austenite at 150°C, resulted in slow and progressive transformation and consequently significantly enhanced TEL.

(3) Increasing strain rate resulted in higher transformation rate at lower strains at RT, but adiabatic heating at higher strains, suppressed transformation appreciably at both temperatures, the effect being much more pronounced at 150°C.

## REFERENCES


1) V. F. Zackay, E. R. Parker and R. Busch: *Trans. Am. Soc. Met.*, **60** (1967), 252.
2) B. C. De Cooman, L. Barbé, J. Mahieu, D. Krizan, L. Samek and M. DeMeyer: Proc. of Int. Symp. on Transformation and Deformation Mechanisms in Advanced High-Strength Steels, ed. by M. Militzer, W. J. Poole and E. Essadiqi, CIM, Montreal, (2003), 5.
3) O. Matsumura, Y. Sakuma and H. Takechi: *Trans. Iron Steel Inst. Jpn.*, **27** (1987), 570.
4) K. Sugimoto, M. Kobayashi and S. Hashimoto: *Metall. Trans. A*, **23A** (1992), 3085.
5) L. Samek, B. C. De Cooman, J. Van Slycken, P. Verleysen and J. Degrieck: Proc. of Int. Symp. on Transformation and Deformation Mechanisms in Advanced High-Strength Steels, ed. by M. Militzer, W. J. Poole and E. Essadiqi, CIM, Montreal, (2003), 77.
6) K. Sugimoto, M. Misu, M. Kobayashi and S. Hashimoto: *ISIJ Int.*, **33** (1993), 775.
7) K. Sugimoto, T. Iida, J. Sakaguchi and T. Kashima: *ISIJ Int.*, **40** (2000), 902.
8) K. Sugimoto, A. Kanda, R. Kikuchi, S. Hashimoto, T. Kashima and S. Ikeda: *ISIJ Int.*, **42** (2002), 910.
9) S. Traint, A. Pichler, M. Blaimschein, B. Röthler, C. Krempaszky and E. Werner: Proc. Int. Conf. on Advanced High Strength Sheet Steels for Automotive Applications, AIST, Warrendale, PA, (2004), 79.
10) S. Hashimoto, S. Ikeda, K. Sugimoto and S. Miyake: *ISIJ Int.*, **44** (2004), 1590.
11) B. D. Cullity: Elements of X-ray Diffraction, Addison-Wesley Publishing Co, Inc., Reading, Massachusetts, (1967), 391.
12) D. J. Dyson and B. Holmes: *J. Iron Steel Inst.*, **208** (1970), 469.
13) G. Frommeyer, U. Brux and P. Neumann: *ISIJ Int.*, **43** (2003), 438.
14) B. Sundman, B. Janssen and J. O. Anderson: *Calphad*, **9** (1985), 153.
15) H. K. D. H. Bhadeshia: Bainite in Steels, University Press, Cambridge, (1992), 63.
16) Y. K. Lee, H. C. Shin, D. S. Leem, J. Y. Choi, W. Jin and C. S. Choi: *Mater. Sci. Technol.*, **19** (2003), 393.
17) P. J. Jacques: *Curr. Opinion Solid State Mater. Sci.*, **8** (2004), 259.
18) K. Sugimoto, A. Nagasaka, M. Kobayashi and S. Hashimoto: *ISIJ Int.*, **39** (1999), 56.
19) G. B. Olson and M. Arzin: *Metall. Trans. A*, **9A** (1978), 713.
20) G. E. Dieter: Mechanical Metallurgy, SI Metric Ed., McGraw Hill Book Company, Singapore, (1988), 275.